NATIONAL ADVISORY COMMITTEE FOR AERONAUTICS

12%
25%
35%

REPORT No. 708

c. 3

TESTS OF THE NACA 0025 AND 0035 AIRFOILS IN THE FULL-SCALE WIND TUNNEL

By W. KENNETH BULLIVANT

1941

For sale by the Superintendent of Documents, Washington, D. C. - - - - - - - - - - - - - - - Price 10 cents
Subscription price $3 per year

AERONAUTIC SYMBOLS

1. FUNDAMENTAL AND DERIVED UNITS

	Symbol	Metric		English	
		Unit	Abbreviation	Unit	Abbreviation
Length	l	meter	m	foot (or mile)	ft (or mi)
Time	t	second	s	second (or hour)	sec (or hr)
Force	F	weight of 1 kilogram	kg	weight of 1 pound	lb
Power	P	horsepower (metric)		horsepower	hp
Speed	V	kilometers per hour	kph	miles per hour	mph
		meters per second	mps	feet per second	fps

2. GENERAL SYMBOLS

W Weight $=mg$

g Standard acceleration of gravity $=9.80665$ m/s^2 or 32.1740 ft/sec^2

m Mass $=\frac{W}{g}$

I Moment of inertia $=mk^2$. (Indicate axis of radius of gyration k by proper subscript.)

μ Coefficient of viscosity

ν Kinematic viscosity

ρ Density (mass per unit volume)

Standard density of dry air, 0.12497 kg-m^{-4}-s^2 at 15° C and 760 mm; or 0.002378 lb-ft^{-4} sec^2

Specific weight of "standard" air, 1.2255 kg/m^3 or 0.07651 lb/cu ft

3. AERODYNAMIC SYMBOLS

S Area

S_w Area of wing

G Gap

b Span

c Chord

A Aspect ratio, $\frac{b^2}{S}$

V True air speed

q Dynamic pressure, $\frac{1}{2}\rho V^2$

L Lift, absolute coefficient $C_L=\frac{L}{qS}$

D Drag, absolute coefficient $C_D=\frac{D}{qS}$

D_0 Profile drag, absolute coefficient $C_{D_0}=\frac{D_0}{qS}$

D_i Induced drag, absolute coefficient $C_{D_i}=\frac{D_i}{qS}$

D_p Parasite drag, absolute coefficient $C_{D_p}=\frac{D_p}{qS}$

C Cross-wind force, absolute coefficient $C_C=\frac{C}{qS}$

i_w Angle of setting of wings (relative to thrust line)

i_t Angle of stabilizer setting (relative to thrust line)

Q Resultant moment

Ω Resultant angular velocity

R Reynolds number, $\rho\frac{Vl}{\mu}$ where l is a linear dimension (e.g., for an airfoil of 1.0 ft chord, 100 mph, standard pressure at 15° C, the corresponding Reynolds number is 935,400; or for an airfoil of 1.0 m chord, 100 mps, the corresponding Reynolds number is 6,865,000)

α Angle of attack

ϵ Angle of downwash

α_0 Angle of attack, infinite aspect ratio

α_i Angle of attack, induced

α_a Angle of attack, absolute (measured from zero-lift position)

γ Flight-path angle

REPORT No. 708

TESTS OF THE NACA 0025 AND 0035 AIRFOILS IN THE FULL-SCALE WIND TUNNEL

By W. KENNETH BULLIVANT

Langley Memorial Aeronautical Laboratory

NATIONAL ADVISORY COMMITTEE FOR AERONAUTICS

HEADQUARTERS, NAVY BUILDING, WASHINGTON, D. C.

Created by act of Congress approved March 3, 1915, for the supervision and direction of the scientific study of the problems of flight (U. S. Code, Title 50, Sec. 151). Its membership was increased to 15 by act approved March 2, 1929. The members are appointed by the President, and serve as such without compensation.

TECHNICAL COMMITTEES

AERODYNAMICS
POWER PLANTS FOR AIRCRAFT
AIRCRAFT MATERIALS

AIRCRAFT STRUCTURES
AIRCRAFT ACCIDENTS
INVENTIONS AND DESIGNS

Coordination of Research Needs of Military and Civil Aviation

Preparation of Research Programs

Allocation of Problems

Prevention of Duplication

Consideration of Inventions

LANGLEY MEMORIAL AERONAUTICAL LABORATORY

LANGLEY FIELD, VA.

AMES AERONAUTICAL LABORATORY

MOFFETT FIELD, CALIF.

Conduct, under unified control, for all agencies, of scientific research on the fundamental problems of flight.

OFFICE OF AERONAUTICAL INTELLIGENCE

WASHINGTON, D. C.

Collection, classification, compilation, and dissemination of scientific and technical information on aeronautics

REPORT No. 708

TESTS OF THE NACA 0025 AND 0035 AIRFOILS IN THE FULL-SCALE WIND TUNNEL

By W. Kenneth Bullivant

SUMMARY

An investigation was conducted in the NACA full-scale wind tunnel to determine the aerodynamic characteristics of the 6- by 36-foot rectangular NACA 0025 and 0035 airfoils. The aerodynamic characteristics of the plain airfoils with rounded and square tips were determined by force tests through a complete angle-of-attack range, including the angles for minimum drag and maximum lift; in addition, the profile drag was determined by the momentum method. The transition points on the airfoils were located by boundary-layer determinations with small total-head and static tubes. Each airfoil was also tested with a 0.20c full-span split flap. Tuft surveys were included to show the progressive breakdown of flow with increasing angles of attack. Previously published data from tests of the NACA 0009, 0012, and 0018 airfoils in the full-scale tunnel have been included in the summary curves.

Within the range covered, the section profile-drag coefficients of the NACA 0025 and 0035 airfoils were practically independent of Reynolds number, the values of these coefficients for the two airfoils being 0.0082 and 0.0112, respectively. With the airfoils equipped with 0.20c full-span split flaps and at a Reynolds number of 3,000,000, the maximum lift coefficient of the NACA 0025 airfoil was 2.57 and that of the NACA 0035 airfoil was 2.54. Tuft and momentum surveys indicated poor flow beginning at a low lift coefficient near the trailing edges of the NACA 0025 and 0035 airfoils. When based on the projected frontal area, the section with the lowest profile-drag coefficient was found to have a thickness approximately 30 percent of the chord.

INTRODUCTION

Reports based on tests of the NACA 0009, 0012, and 0018 airfoils in the full-scale wind tunnel at the Langley Memorial Aeronautical Laboratory were published in 1938 and 1939. (See references 1, 2, and 3.) The accuracy of these data has been widely accepted, and in some instances they have been used as a standard in determining corrections for smaller wind tunnels. The present report of the NACA 0025 and 0035 airfoil tests extends the data of this particular airfoil series to a thickness ratio beyond which there is little likelihood of flight application. A test procedure similar to that used for testing the three thinner airfoils (references 1 and 2) was followed. This procedure includes momentum and boundary-layer determinations and tuft surveys for the plain airfoils and the determination of the aerodynamic characteristics of the airfoils equipped with 0.20c full-span split flaps. The Reynolds number range for the tests was from 1,400,000 to 5,900,000. Data from references 1, 2, and 3 have been included in several graphs and in a table listing important characteristics of the airfoils of this symmetrical series.

SYMBOLS

The symbols used in the report are defined as follows:

α	angle of attack of airfoil
α_0	angle of attack for infinite aspect ratio
C_L	airfoil lift coefficient
c_l	section lift coefficient
$\frac{dC_L}{d\alpha}$	slope of airfoil lift curve, per degree
a_0	slope of lift curve for infinite aspect ratio, per degree
C_D	airfoil drag coefficient
C_{D_0}	airfoil profile-drag coefficient
c_{d_0}	section profile-drag coefficient
L/D	ratio of lift to drag
$C_{m_{c/4}}$	pitching-moment coefficient about quarter-chord point of airfoil
$c_{m_{a.c.}}$	section pitching-moment coefficient about aerodynamic center of plain airfoil
A	aspect ratio
σ	a factor used to correct induced drag to allow for the change from elliptical span loading to a span loading for an airfoil with rectangular plan form (0.051)
δ_f	flap deflection
u	local velocity, feet per second
U	velocity at edge of boundary layer, feet per second
V	tunnel air speed
y	distance normal to surface of airfoil; and distance above center of wake
p	local static pressure

q_0	free-stream dynamic pressure $\left(\frac{1}{2}\rho V^2\right)$
c	airfoil chord
s	distance along airfoil surface from theoretical stagnation point
x	distance along chord from leading edge of chord
t	wing thickness
H_0	free-stream total pressure
H_1	total pressure in wake
p_0	free-stream static pressure
F	a factor, usually about 0.8 to 0.9
R	Reynolds number

EQUIPMENT AND AIRFOILS

A description of the NACA full-scale wind tunnel and of its test equipment is given in reference 4. The turbulence factor of the tunnel as determined by sphere tests is 1.1 (reference 5). The 6- by 36-foot rectangular NACA 0025 and 0035 airfoils (see figs. 1 and 2) were of steel-spar construction with ribs at 12-inch intervals. The airfoils were covered with $\frac{1}{16}$-inch aluminum sheets, attached with countersunk screws. The exterior seams and the screw slots were filled; and the entire surface was sanded, coated with paint primer, and then resanded with fine water sandpaper to a finish considered to be aerodynamically smooth. Surface waviness was reduced to a minimum for this type of construction. The maximum variation from the true section ordinates was $\pm\frac{1}{16}$ inch, but over most of the surface a smaller tolerance was adhered to. Detachable

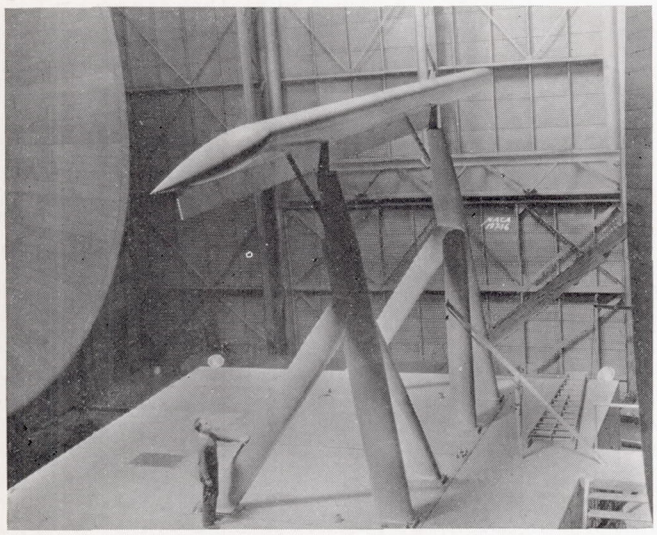

FIGURE 1.—The NACA 0025 rounded-tip airfoil with a 0.20c full-span split flap mounted in the full-scale wind tunnel.

rounded tips were provided for each airfoil. These tips formed one-half of a solid of revolution, the radius at each chordwise station being equal to one-half of the local airfoil thickness. (See fig. 1.)

A full-span 0.20c split flap was used with each airfoil. The flap was constructed of $\frac{1}{2}$-inch plywood with braces at several points along the span to provide deflections from 15° to 90°. (See fig. 1.) The flap deflection δ_f was measured between the lower surface of each airfoil and the flap; the hinge point was so located that the trailing edges of the airfoil and the flap would coincide when the flap was undeflected.

The rake used for the momentum determinations

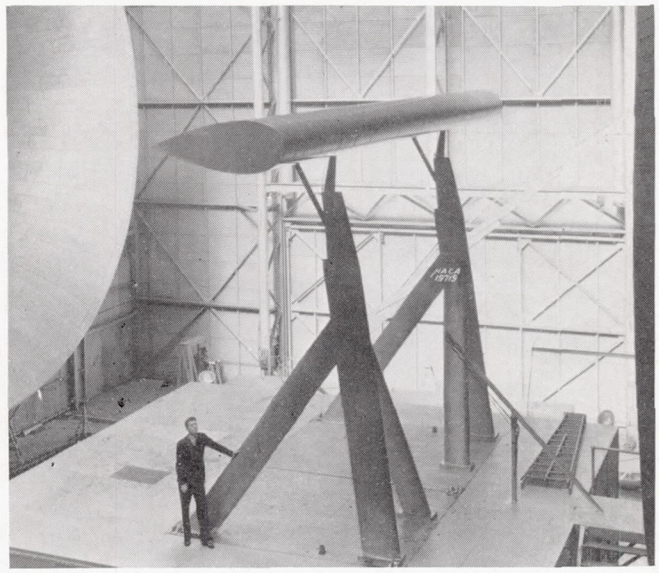

FIGURE 2.—The NACA 0035 airfoil with rounded tips removed.

consisted of a comb of 37 small total-head tubes and a comb of 13 static-pressure tubes spaced 6 inches laterally. (See fig. 3.) The rake was mounted on the survey apparatus (see reference 4) and each tube was connected to a multiple-tube manometer carried in the survey carriage above the jet. A sketch of the rake is given in reference 3.

The velocities at four heights above the surface of the airfoils were determined by a bank of four small total-head tubes and one static tube (fig. 4). The tubes were of stainless steel, 0.040-inch outside diameter, with a 0.003-inch wall thickness. The front ends of the total-head tubes were flattened to an outside thickness of 0.012 inch for a length of 1 inch from the opening. Each tube was bent to conform to the airfoil contour and the height was set with a templet-type gage. At the conclusion of each test, the heights of the tubes were again measured with a thickness gage. Pressures were transmitted through small tubing taped along the trailing edges of the airfoils and down the supporting struts to a manometer located in the balance room. Readings were taken simultaneously at four chordwise stations with the banks of tubes spaced laterally to eliminate interference effects.

TESTS

During the tests the airfoils were mounted with the main supports attached at the quarter-chord line of the

airfoils (figs. 1 and 2). The angle of attack was changed by a vertical movement of the lower ends of the rear strut members.

Lift, drag, and pitching moments of each airfoil were obtained at an average test velocity of 57 miles per hour,

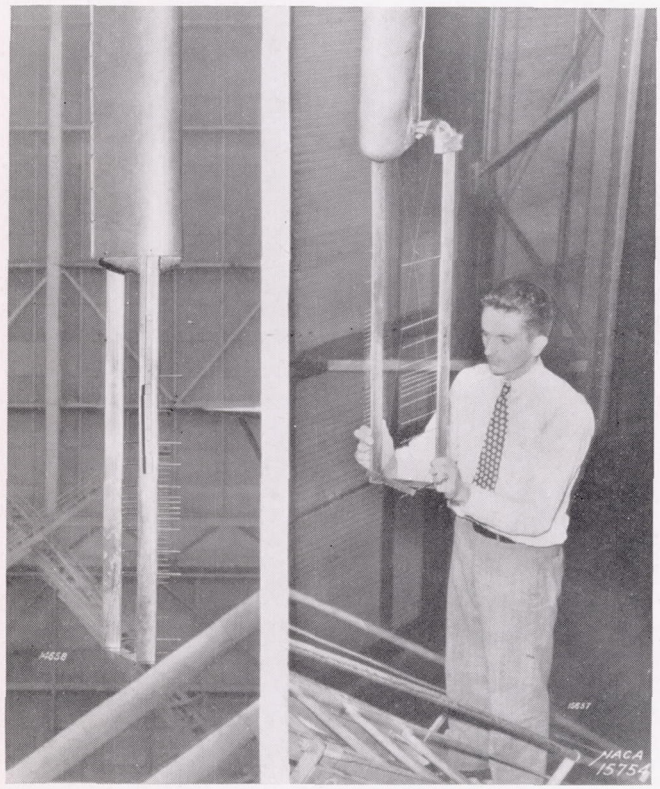

FIGURE 3.—Views of the rake used for momentum determinations.

corresponding to a Reynolds number of 3,200,000, and through an angle-of-attack range beginning at −8° and extending through maximum lift for the following test conditions: square-tip with flap undeflected; rounded-tip with flap undeflected; and rounded-tip with flap deflected 15°, 30°, 45°, 60°, 75°, and 90°. The effect of the Reynolds number on minimum drag and maximum lift for the rounded-tip and the square-tip airfoils and on maximum lift for the rounded-tip airfoils with flap deflected 60° was determined at velocities up to 105 miles per hour (R=5,900,000) for the minimum drag coefficients and 76 miles per hour (R=4,300,000) for the maximum lift coefficients. Wool tufts were used on the upper surface of each rounded-tip airfoil to show the progressive breakdown of flow with increasing angles of attack.

By means of the rake previously described, simultaneous measurements were made of the total and the static pressures 20 percent of the chord behind the trailing edge of each airfoil at 27 spanwise locations. The measurements were made at five lift coefficients from −0.5 to 0.5.

At three angles of attack, corresponding to a small negative lift coefficient, zero lift coefficient, and a small positive lift coefficient, and at tunnel speeds from 30 to 90 miles per hour (R ranging from 1,700,000 to 5,100,000), the velocities at effective heights of 0.008, 0.031, 0.046, and 0.156 inch above each airfoil surface were measured. The banks of small total-pressure and static-pressure tubes were used, and determinations were made at 0.05c intervals from the 0.05c to the 0.50c position.

REDUCTION OF DATA

The general method outlined in reference 1 for the correction of force-test data and the conversion to infinite-aspect-ratio characteristics has been followed. In the computation of the coefficients for the airfoils with the rounded tips, the added area of the tips was not included. All coefficients for an aspect ratio of 6 listed in this report are thus based on the same area—that of the square-tip airfoils.

A separate determination of the support tare and the interference drags by force tests was not made as in the case of the thinner airfoils of this series reported in reference 1. For the correction of all the force-test results, a combined tare, interference, and horizontal-

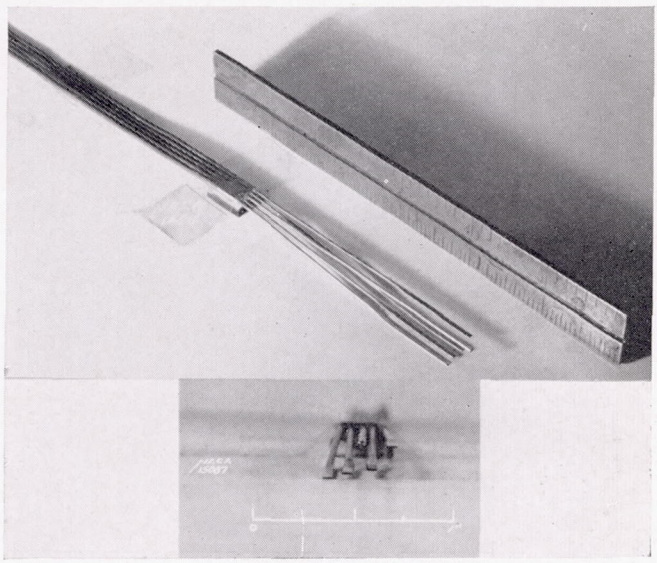

FIGURE 4.—Bank of total-head tubes and static tube used for boundary-layer surveys.

buoyancy correction was evaluated by a direct comparison, at several low lift coefficients, of the drag coefficients obtained by the force tests and the momentum method. The profile-drag coefficient as determined by the momentum method was obtained by spanwise integration of the section profile-drag coefficients. All of the measured values were used except those obviously affected by the supporting struts; thus a coefficient was obtained that excluded the effect of the supports. No lift correction for the supports was made because

previous tests in the full-scale tunnel have shown that this correction is negligible. The following formula

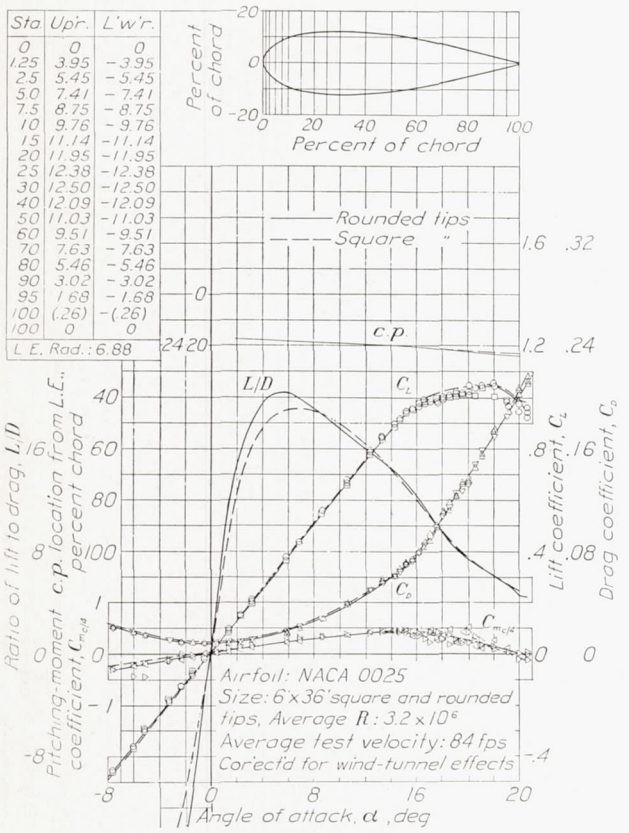

FIGURE 5.—Characteristics of NACA 0025 airfoil of aspect ratio 6.

was used in computing the combined tare, interference, and buoyancy correction for each airfoil:

$$C_{D_t}=\left[C_{D_N}-\left(\frac{C_L^2}{\pi A}\right)(1+\sigma)\right]-C_{D_0}$$

where

C_{D_t} tare-interference-buoyancy coefficient

C_{D_N} gross drag coefficient of the airfoil with rounded tips corrected only for stream-angle and jet-boundary effects (See reference 1.)

C_{D_0} profile-drag coefficient of the airfoil with rounded tips from momentum survey

The tare-interference-buoyancy coefficient C_{D_t} for the NACA 0025 and 0035 airfoils at zero lift amounted to 0.0029 and 0.0046, respectively, which is slightly greater than one-third the minimum drag of each airfoil. The portion of the C_{D_t} and to buoyancy was determined for each airfoil from static-pressure surveys in the test plane and was found to be 0.0007 for the NACA 0025 airfoil and 0.0010 for the NACA 0035 airfoil. The C_{D_t} values decreased rapidly with increasing angles of attack and at 7° (the highest positive angle at which momentum determinations were made) approached constant values of 0.002 for the NACA 0025 airfoil and 0.003 for the NACA 0035 airfoil; these values were used for the higher angles of attack.

The foregoing method of determining the effect of the supports on the airfoil drag does not permit an accurate pitching-moment correction; therefore this correction was not applied. Because previous tests have shown that very small pitching-moment corrections are due to these supports and because the pitching-moment coefficient curves for the airfoils used in the present investigation pass through zero at zero angle of attack (figs. 5 and 6), the error due to the omission of this correction is believed to be negligible. The factor F was obtained by substitution of the proper wake characteristics in figure 7 of reference 6. The free-stream dynamic pressure q_0, or H_0-p_0, was obtained in the usual manner from tunnel calibrations.

In order to check the section profile-drag coefficients as determined by the foregoing simplified method involving the use of the F factor, computations were also made by the longer, more rigorous method outlined in reference 3 for the NACA 0035 airfoil, and exact agreement resulted. The true section profile drag of each airfoil was considered to be an average of the values obtained by the momentum method over the

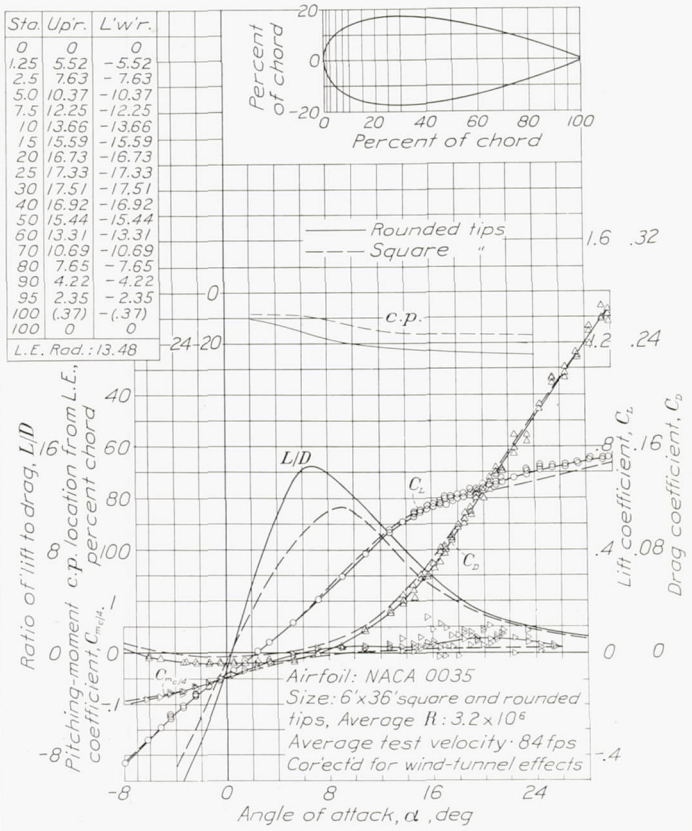

FIGURE 6.—Characteristics of NACA 0035 airfoil of aspect ratio 6.

middle 28 feet of the span exclusive of the values affected by the struts and the local flow disturbances.

The boundary-layer test data have been presented in the same form as that employed in reference 2 so

that the graphs for the NACA 0009, 0012, and 0018 airfoils might be compared directly with those for the NACA 0025 and 0035 airfoils of this report.

PRECISION

The accuracy of the basic measurements is believed to be within the following limits:

α	$\pm 0.1°$
$C_{L_{max}}$	± 0.05
C_{D_0}	± 0.0004 $(C_L=0)$
$C_{m_{c/4}}$	± 0.010

RESULTS AND DISCUSSION

Force and momentum tests.—The principal aerodynamic characteristics of the NACA 0025 and 0035 rounded- and square-tip airfoils of aspect ratio 6 are given in figures 5 and 6 for an average Reynolds number of 3,200,000. Although curves for both rounded-tip and square-tip airfoils are shown, the test points for the square-tip condition are not included. The corresponding section characteristics are presented in figure 7. The fact that the lift curve of the NACA 0035 airfoil does not pass through zero at 0° angle of attack can be accounted for by a slight strut interference effect on the lift, which has been disregarded in these tests.

Figures 8 and 9 show the progression of the stall with increasing angles of attack, as determined by tufts taped on the upper surfaces of the airfoils. The cross-hatching indicates a reverse flow or a haphazard motion of the tufts. The row of tufts nearest the trailing edge showed a slight disturbance on each airfoil even at zero lift.

The effect of Reynolds number on the maximum lifts of the plain and the flapped airfoils is shown in figure 10. In the range investigated there was an increase in maximum lift with increasing Reynolds number except for the NACA 0035 rounded-tip airfoil between Reynolds numbers of 1,600,000 and 3,100,000, where the effect was noticeably reversed. The minimum drag of the airfoils with rounded and square tips is shown in figure 11 to be practically unaffected by Reynolds number change.

The section profile drag as determined by the momentum method at 27 spanwise locations is shown in figure 12 for three of the angles of attack at which the determinations were made. The local drag increase near the midspan of the airfoils might be explained by an increased turbulence of the jet in this region. Sphere tests (reference 5) showed the stream turbulence to be considerably greater at the tunnel center line than at a station one-fourth of jet width out from the center line.

The C_{D_0} values previously mentioned for correcting all the force-test drag data were those obtained by integration of the curves in figure 12 across the full span including the tips. With disregard of the large local effects and with an average taken over the middle 28 feet of the airfoil spans (dashed lines of fig. 12), the section profile-drag coefficients c_{d_0} were obtained. It will be noted that the net effect of the rounded tips on the airfoil drag is slight.

Figures 13, 14, and 15 present summary curves showing the effect of Reynolds number, lift coefficient, and section thickness on the profile drag of NACA

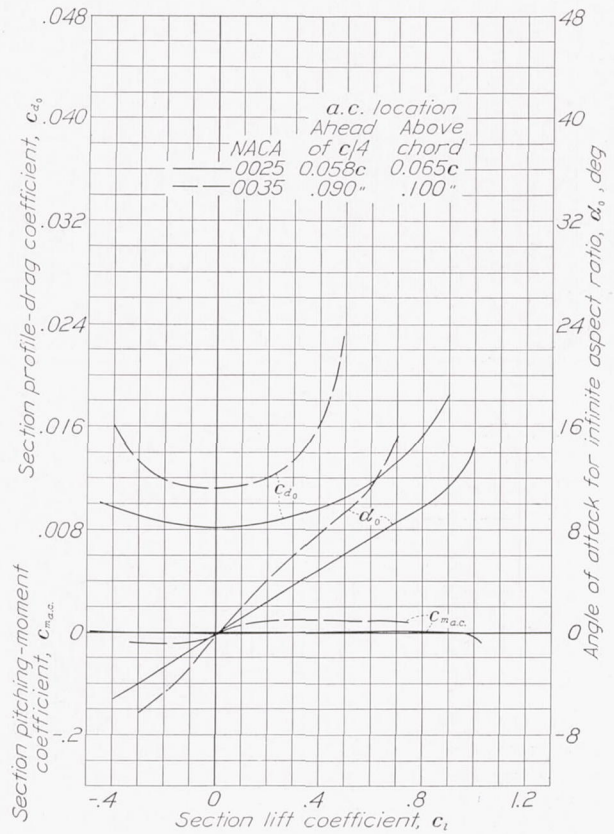

FIGURE 7.—Section characteristics of the NACA 0025 and 0035 airfoils at a Reynolds number of 3,200,000.

symmetrical airfoils between 0009 and 0035. Data from references 1 and 3 have been used in the three figures. The effects of the square tips obtained from the present tests are also included in figure 14. In figure 13, the profile-drag coefficients for the NACA 0025 and 0035 airfoils beyond the range investigated by the momentum method were obtained by deducting the computed induced drag from the drag obtained in the force tests. (See figs. 5 and 6.) The section profile-drag coefficient at a Reynolds number of 5,000,000 is 0.0081 for the NACA 0025 airfoil and 0.0112 for the NACA 0035 airfoil. The profile-drag coefficient increases on a straight line (fig. 14) with airfoil thickness up to 25 percent; after a thickness of 25 percent the coefficient increases more rapidly. It is interesting to note the large amount of drag caused by the square tips on the thicker airfoils. This drag amounts to more than one-fourth the total drag of the NACA 0035 airfoil. In figure 15 is shown the variation of the section drag coefficient at zero lift with Reynolds number for all the symmetrical airfoils tested in the full-scale wind tunnel.

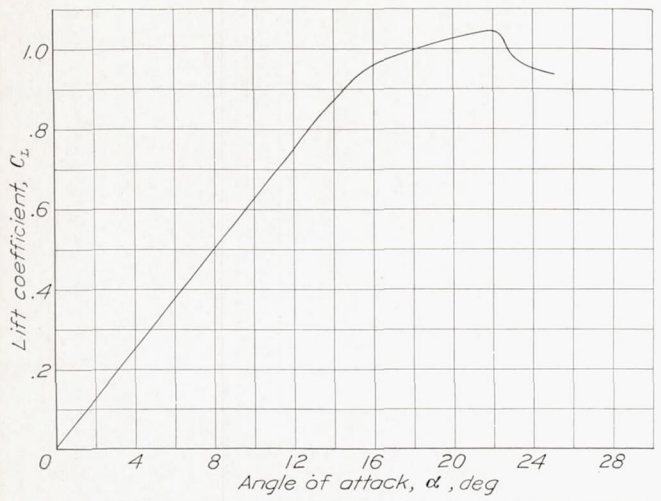

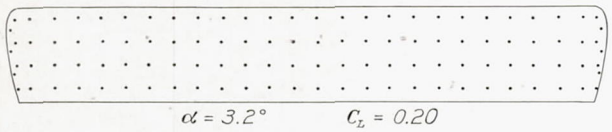

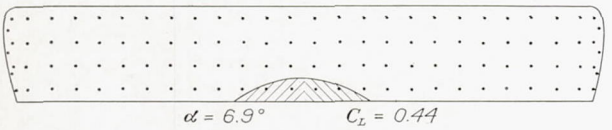

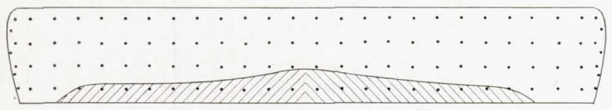

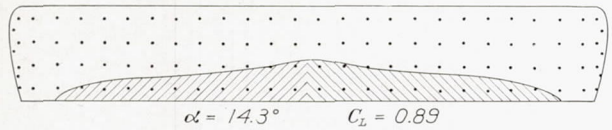

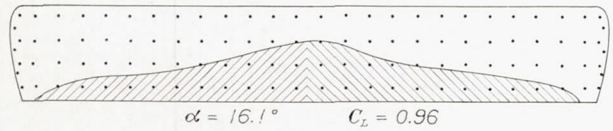

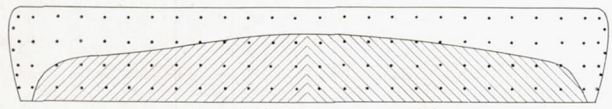

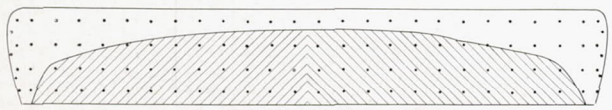

FIGURE 8.—Stalling contours of the NACA 0025 airfoil with rounded tips. Approximate test velocity, 81 feet per second. Cross-hatched areas indicate stalled region.

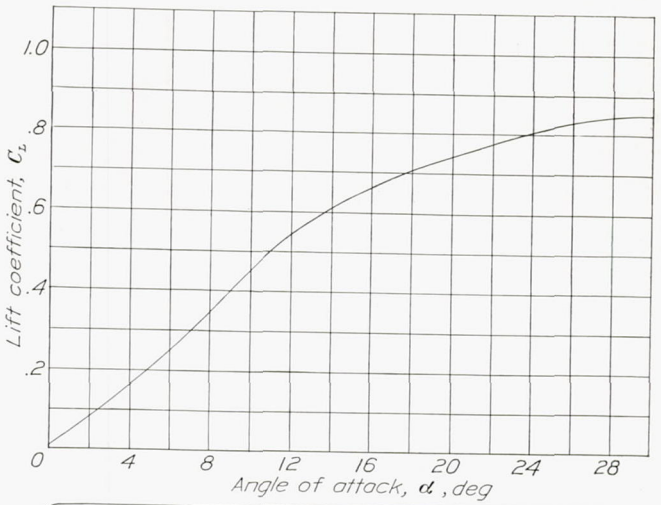

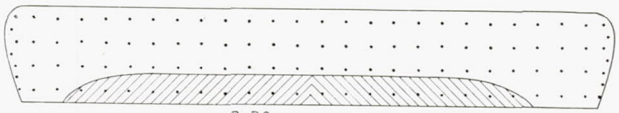

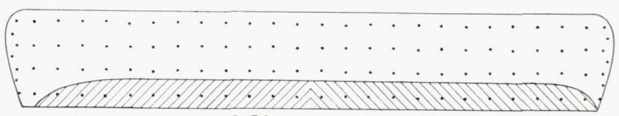

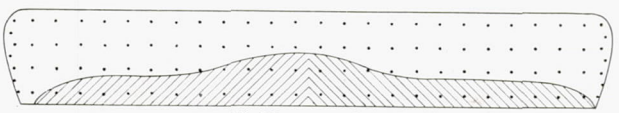

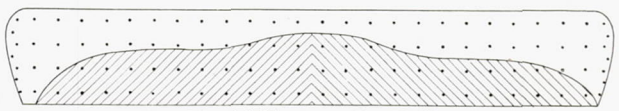

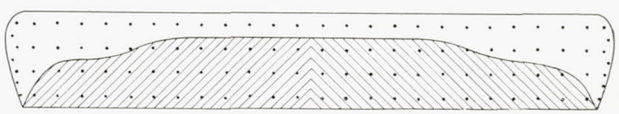

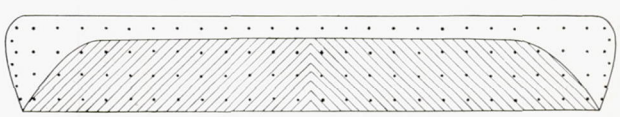

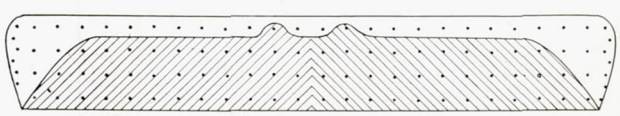

FIGURE 9.—Stalling contours of the NACA 0035 airfoil with rounded tips. Approximate test velocity, 81 feet per second. Cross-hatched areas indicate stalled region.

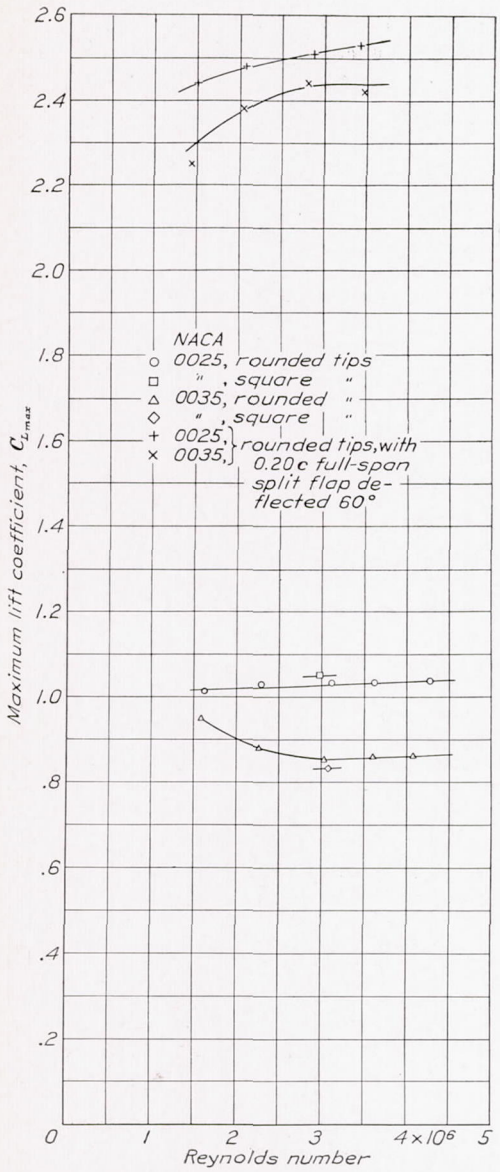

FIGURE 10.—Variation of maximum lift coefficient with Reynolds number for the NACA 0025 and 0035 airfoils of aspect ratio 6.

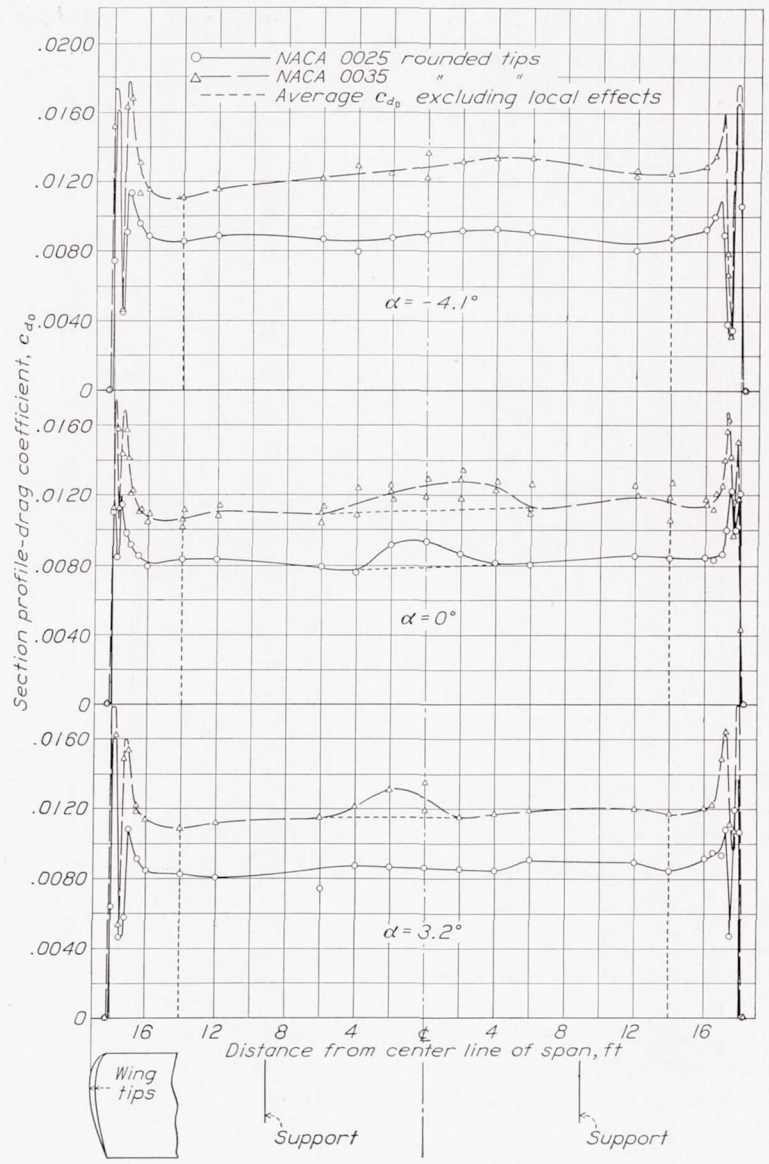

FIGURE 12.—Variation of section profile-drag coefficient across the spans of the two rounded-tip airfoils of aspect ratio 6 at three angles of attack. Reynolds number, 4,400,000.

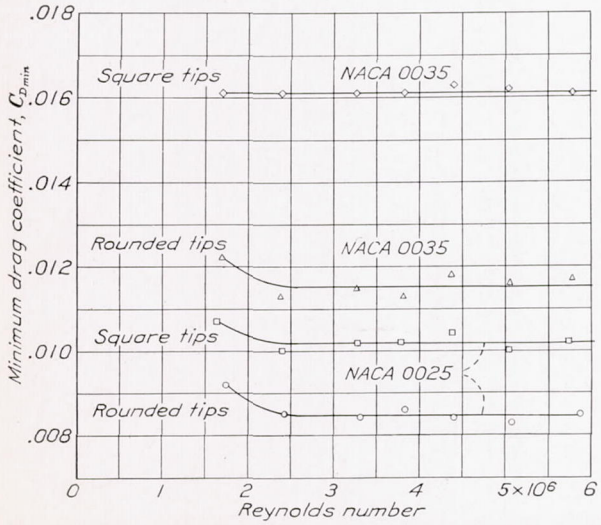

FIGURE 11.—Variation of minimum drag coefficient with Reynolds number for the NACA 0025 and 0035 airfoils of aspect ratio 6.

The characteristics of the NACA 0025 and 0035 rounded-tip airfoils of aspect ratio 6 equipped with 0.20c full-span split flaps and the corresponding infinite-aspect-ratio characteristics are presented in figures 16 to 19. It will be noted in these figures that, for the flapped airfoils, $c_{m_{a.c.}}$ is taken with reference to the aerodynamic center of the plain airfoil. Comparison of the $C_{m_{c/4}}$ and the $c_{m_{a.c.}}$ curves reveals that the pitching moments about the quarter-chord point for the flapped condition are more nearly constant and are of smaller magnitude throughout the angle-of-attack range than those taken about the aerodynamic centers of the plain airfoils.

The effect of a 0.20c full-span split flap on the maximum lifts of the NACA 0025 and 0035 rounded-tip airfoils is shown in figure 20 by curves of the maximum lift coefficient and the increment of maximum lift coefficient against flap angle. The maximum lift coeffi-

294896—41——2

cient for the NACA 0025 airfoil with flaps deflected was 2.57 and for the NACA 0035 airfoil was 2.54, the corresponding flap angles being approximately 75° and 82°, respectively. With these flap-angle settings

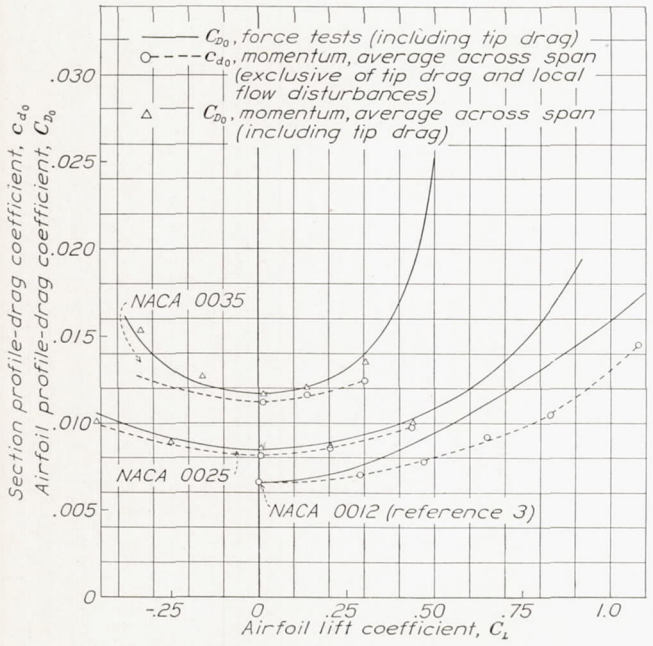

FIGURE 13.—Variation of profile-drag coefficient with lift coefficient obtained from momentum and force tests. Reynolds number, 4,400,000.

the increases in the maximum lift coefficients were 1.54 for the NACA 0025 airfoil and 1.69 for the NACA 0035 airfoil.

In figure 21 data from reference 1 have been included to show the variation of maximum lift coefficient of the plain and the flapped airfoils with airfoil thickness. When equipped with a 0.20c full-span split flap, an airfoil having a thickness between 25 and 30 percent of the chord has the largest lift of this symmetrical series.

The variation of the speed-range index $C_{L_{max}}/C_{D_{min}}$ with airfoil thickness is given in figure 22. If this index is used as a criterion, the optimum thickness for a plain airfoil is between 10 and 12 percent of the chord. The optimum thickness for the flapped condition cannot be accurately stated because of insufficient data. It will be noted, however, that the penalty for increased thickness is not nearly so great for the flapped airfoil as for the plain airfoil. When the section profile-drag coefficient at zero lift (fig. 14) is based on the frontal area, as in figure 23, the drag coefficient becomes a minimum for a thickness ratio of approximately 0.30.

Table I presents a summary of the important characteristics of the NACA 0009, 0012, 0018, 0025, and 0035 airfoils obtained from full-scale wind-tunnel tests.

With the use of the maximum p/q_0 values (later explained in figs. 30 and 31), the limiting speeds due to compressibility have been computed for each of the airfoils according to a method outlined in reference 7. At sea level and at a lift coefficient of 0.3, the estimated critical speeds of the NACA 0025 and 0035 airfoils are 440 and 400 miles per hour, respectively. At alti-

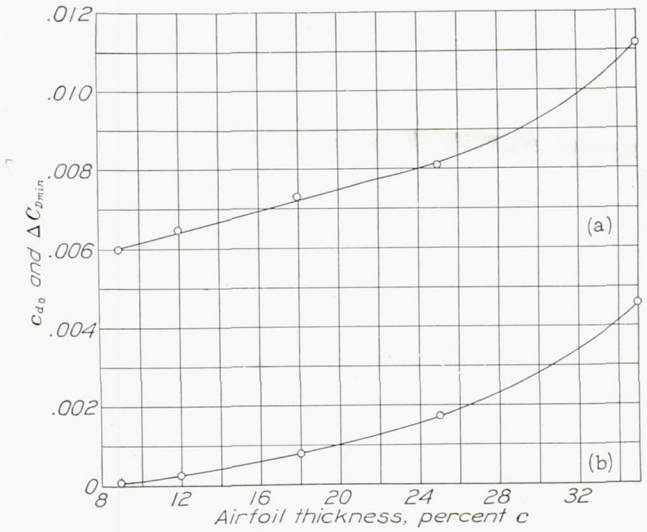

(a) Section profile-drag coefficient at zero lift, c_{d_0}.

(b) $\Delta C_{D_{min}}$ due to square tips.

FIGURE 14.—Variation of section profile-drag coefficient and drag due to square tips with airfoil thickness for NACA symmetrical airfoils. Reynolds number, 5,000,000; C_L, 0. (Data for NACA 0009, 0012, and 0018 airfoils from reference 1.)

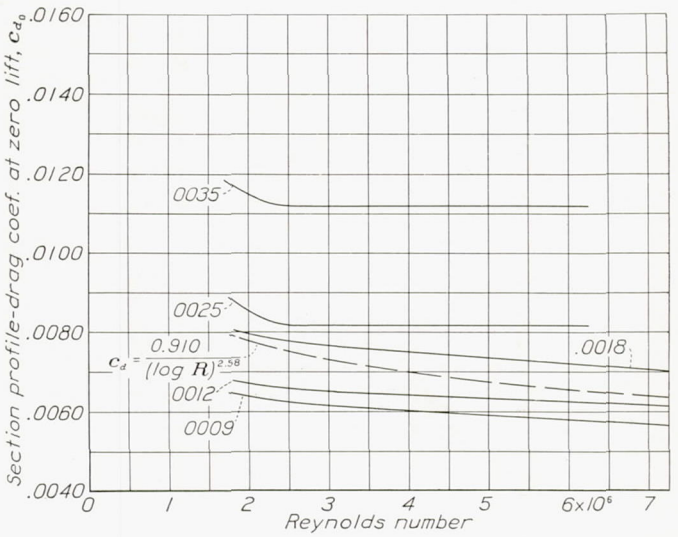

FIGURE 15.—Variation of section profile-drag coefficients at zero lift with Reynolds number for five NACA symmetrical airfoils. (Data for NACA 0009, 0012, and 0018 airfoils from reference 1.)

tudes other than sea level, the critical speeds would be decreased approximately 1.5 miles per hour per thousand feet of altitude. Although the method outlined in reference 7 for obtaining the limiting speeds due to compressibility has been generally used for estimating critical speeds, it has been shown to be somewhat optimistic; consequently, the values listed in table I may be as much as 5 percent higher than would actually be obtained.

The foregoing data indicate that the penalty in drag for airfoil thickness up to 35 percent of the chord is not unreasonably high. It appears that airfoil thicknesses up to 25 percent of the chord might be advantageously incorporated in an airplane design.

Transition measurements.—The location of the transition points on the upper surfaces of the NACA 0025 and 0035 airfoils for several lift coefficients and tunnel speeds was determined from the boundary-layer velocity measurements shown in figures 24 and 25. Table II presents a list of values by which the distance from the theoretical stagnation point along the surface (s/c) is converted to the distance along the chord from the leading edge (x/c). The velocity 0.008 inch above the surface generally decreases with increasing distance from the stagnation point until a minimum is reached; then it rises to a maximum and starts to decrease again. The transition point is defined in this report as the s/c position at which the u/U value begins to increase after the first pronounced minimum is reached. The transition region is considered to be the region of increasing values immediately downstream from the transition point.

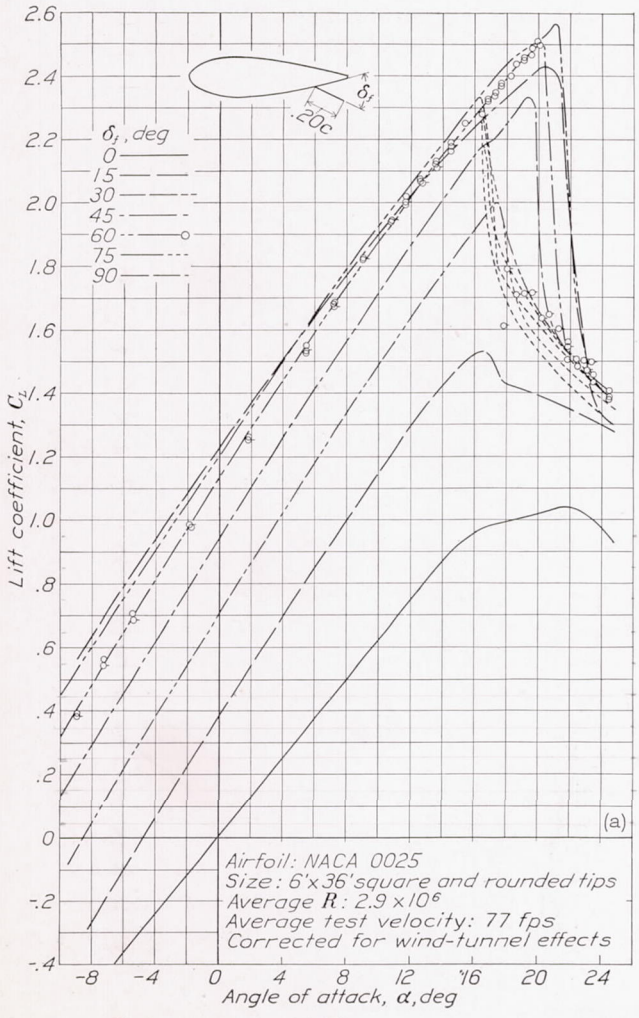

(a) Lift.

FIGURE 16.

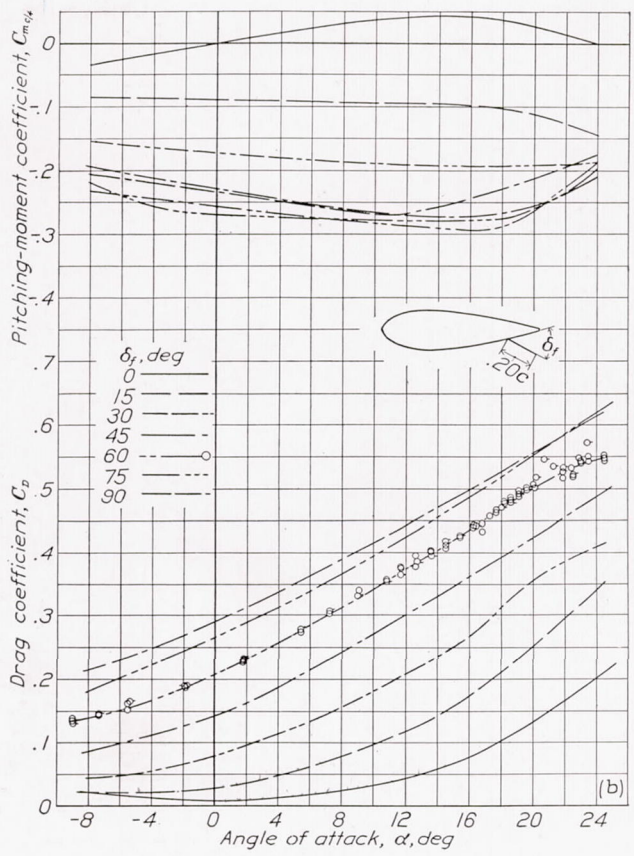

(b) Drag and pitching moment.

FIGURE 16.

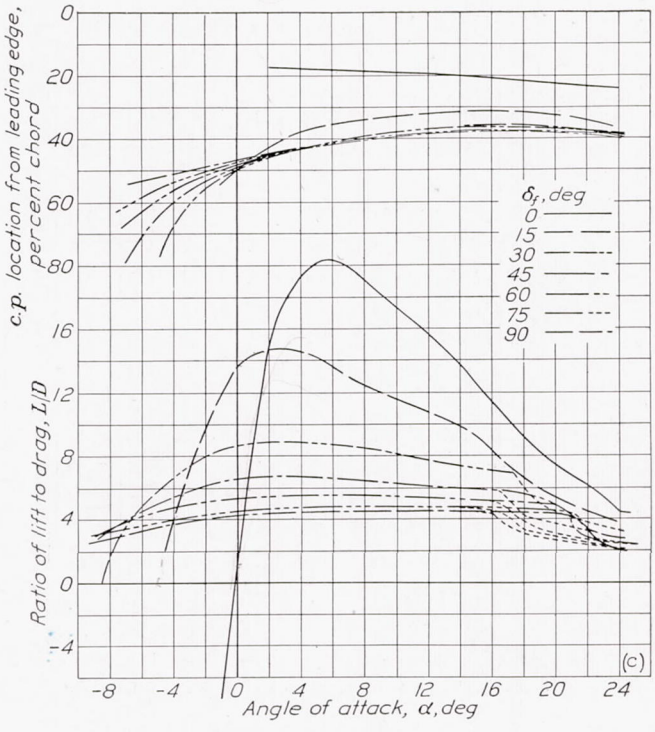

(c) L/D and center of pressure.

FIGURE 16.—Characteristics of the NACA 0025 airfoil of aspect ratio 6 with a 0.20c full-span split flap.

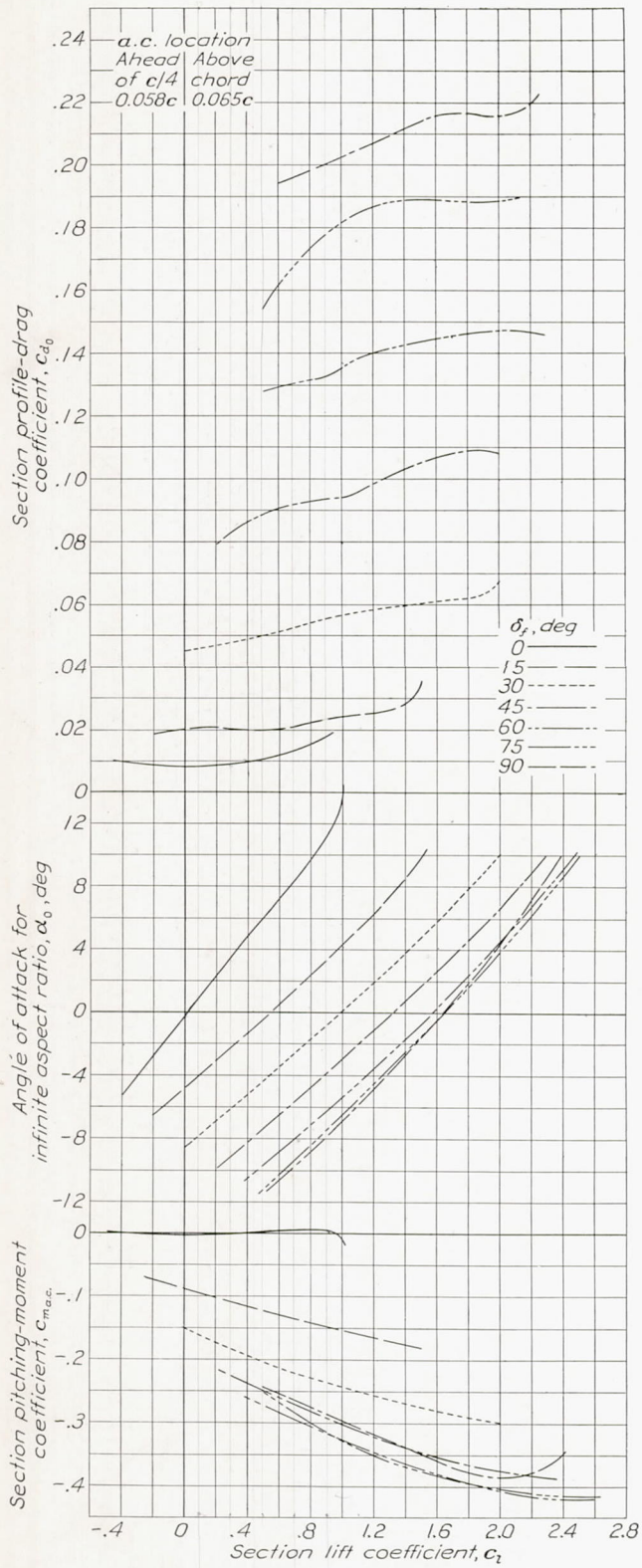

FIGURE 17.—Section characteristics of the NACA 0025 airfoil with a 0.20c full-span split flap at a Reynolds number of 3,000,000.

The transition regions for the negative angles of attack (figs. 24 (a) and 25 (a)) are seen to be poorly

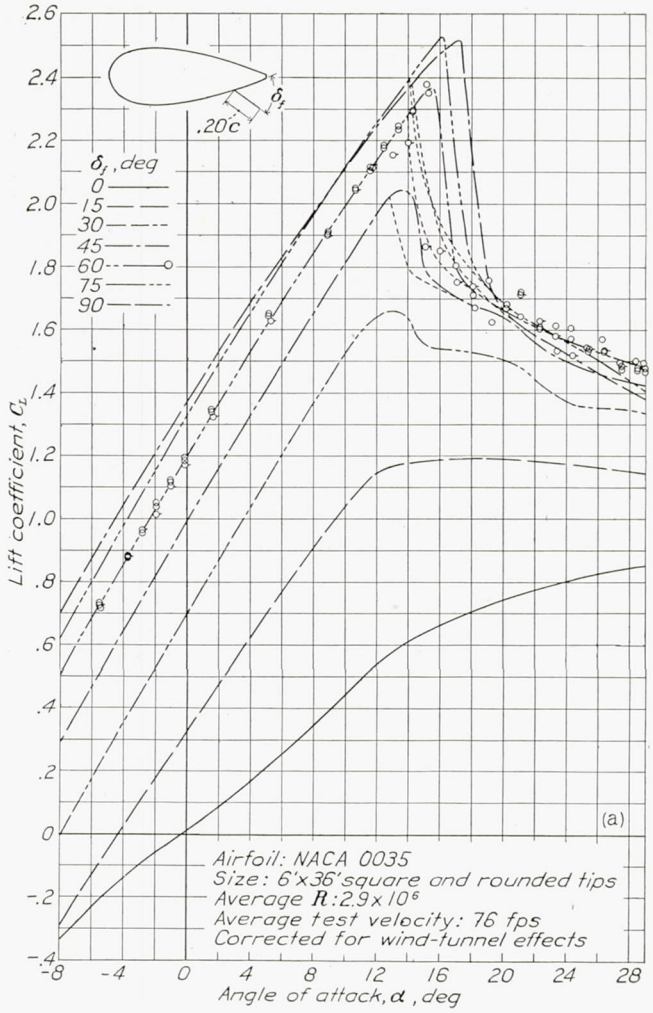

(a) Lift.

FIGURE 18.

defined by the determinations with the tubes nearest the surface. The typical velocity-distribution profiles given in figures 26 and 27 for a Reynolds number of 3,200,000 show that fully developed turbulent profiles were never obtained for the NACA 0025 airfoil at negative lift and only at the s/c position farthest from the stagnation point for the NACA 0035 airfoil.

In figure 24 (c) a tendency is observed for the transition point of the NACA 0025 airfoil at a lift coefficient of 0.49 to become less sharply defined with increasing tunnel velocity and to move far forward at the highest speed obtained. The corresponding velocity-distribution profiles at a Reynolds number of 4,000,000 indicated that the transition point does move ahead to an s/c position of about 0.2. Unfortunately, determinations were not made over the forward portion of the NACA 0025 airfoil at the Reynolds number of 5,100,000.

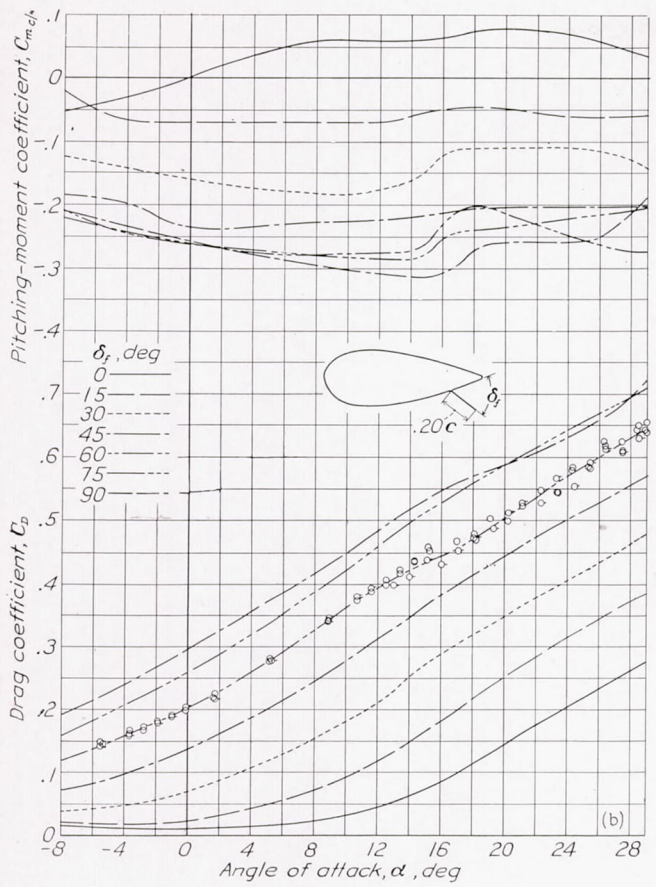

(b) Drag and pitching moment.

FIGURE 18.

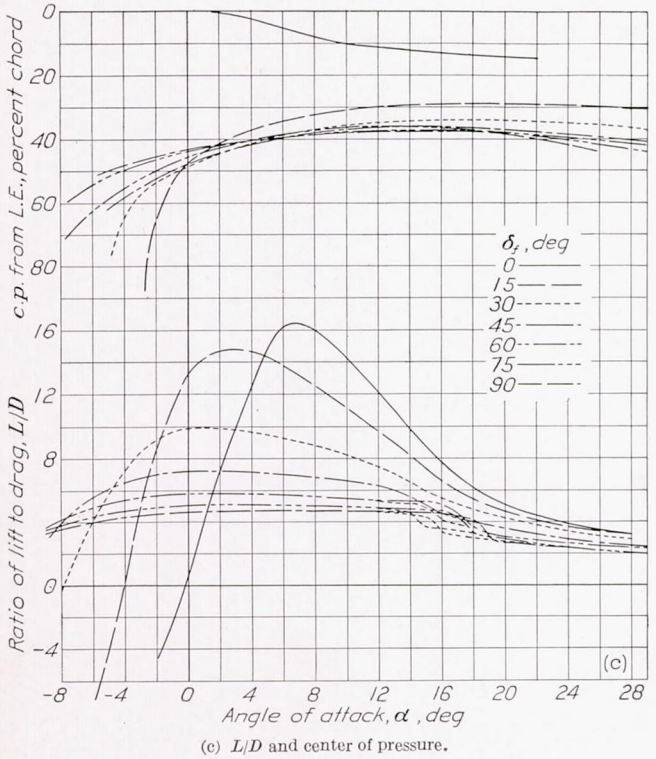

(c) L/D and center of pressure.

FIGURE 18.—Characteristics of the NACA 0035 airfoil of aspect ratio 6 with a 0.20c full-span split flap.

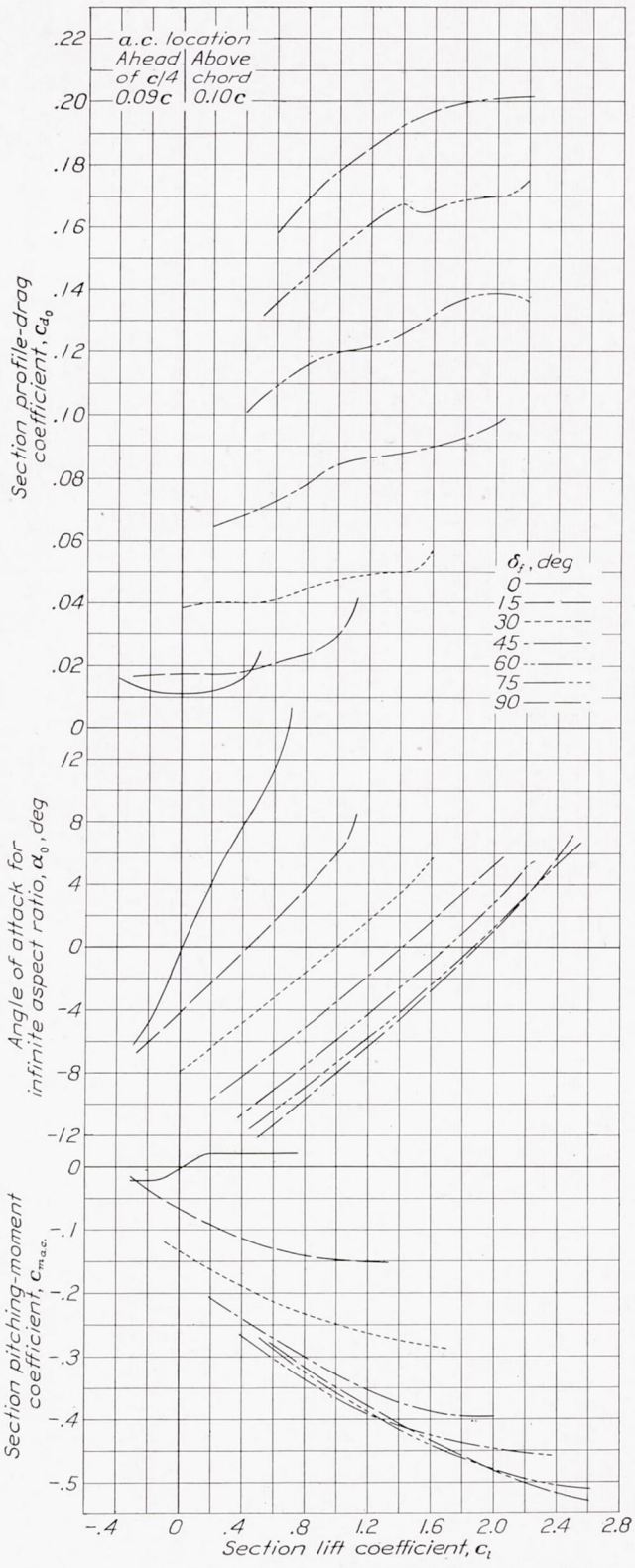

FIGURE 19.—Section characteristics of the NACA 0035 airfoil with a 0.20c with a 0.20c full-span split flap at a Reynolds number of 3,000,000.

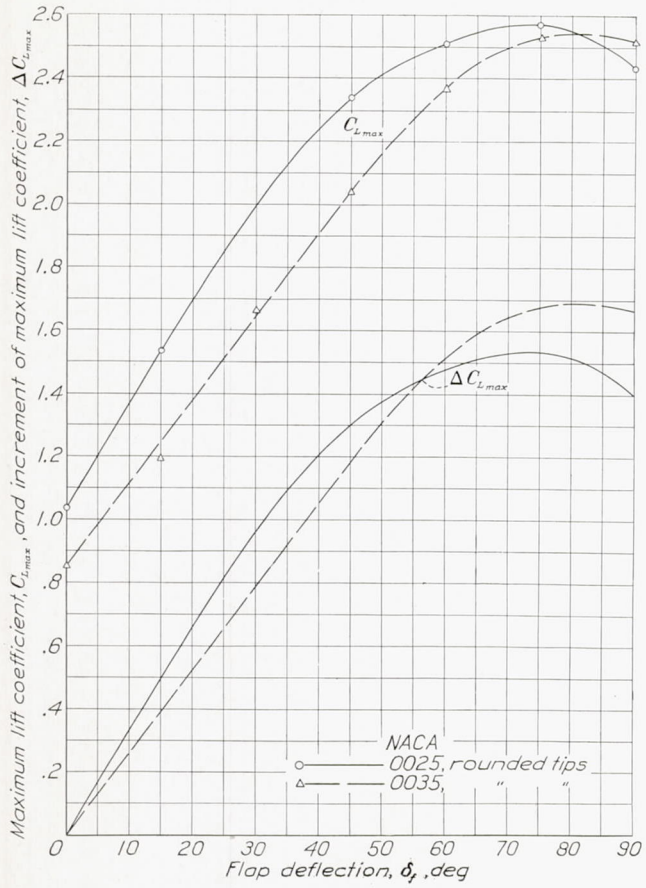

FIGURE 20.—Variation of maximum lift coefficient and increment of maximum lift coefficient with flap deflection for two NACA airfoils. Reynolds number, 3,000,000; aspect ratio, 6.

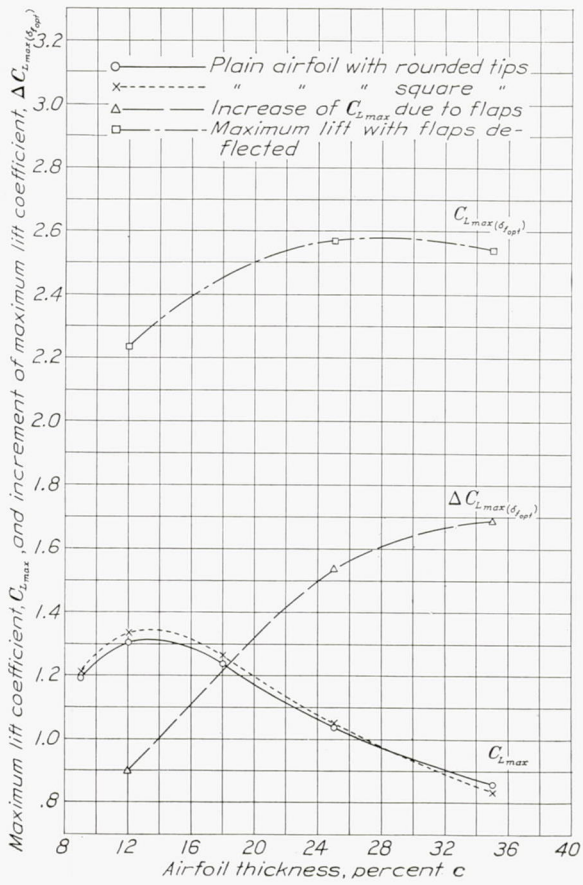

FIGURE 21.—Variation of maximum lift coefficient for an airfoil, with and without flaps, and increment of maximum lift coefficient due to flaps with airfoil thickness for three NACA airfoils. Reynolds number, 3,000,000; aspect ratio, 6. (Data for NACA 0009, 0012, and 0018 airfoils from reference 1.)

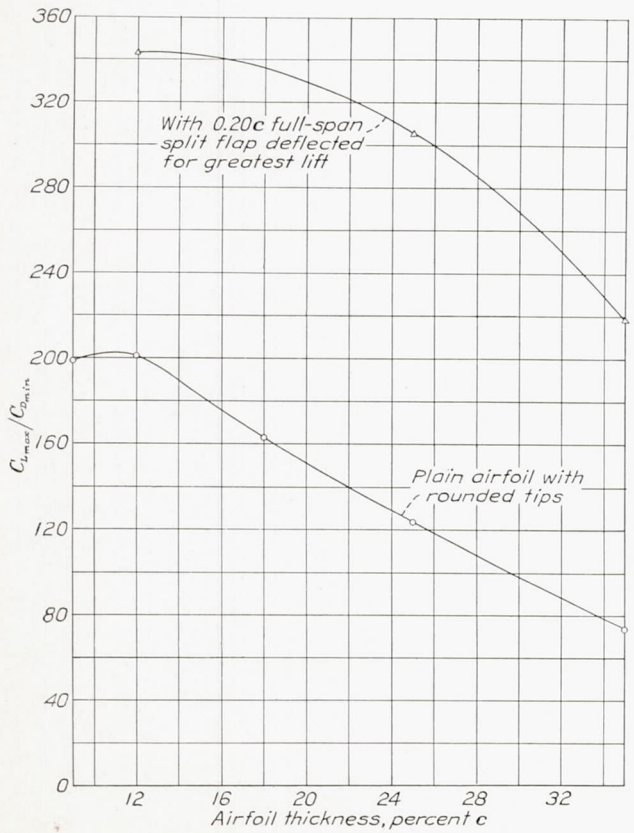

FIGURE 22.—Variation of $C_{L_{max}}/C_{D_{min}}$ with airfoil thickness for NACA symmetrical series.

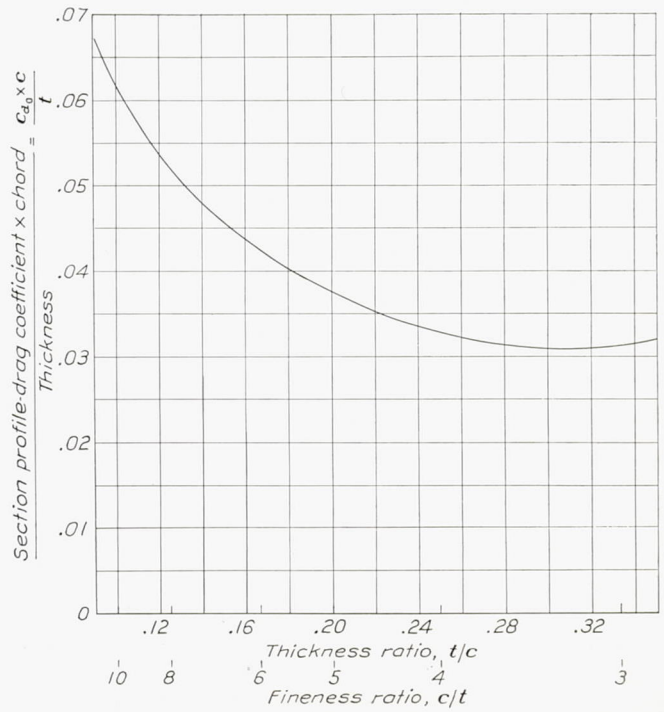

FIGURE 23.—Variation of section profile-drag coefficient (based on thickness) with thickness ratio. Reynolds number, 5,000,000.

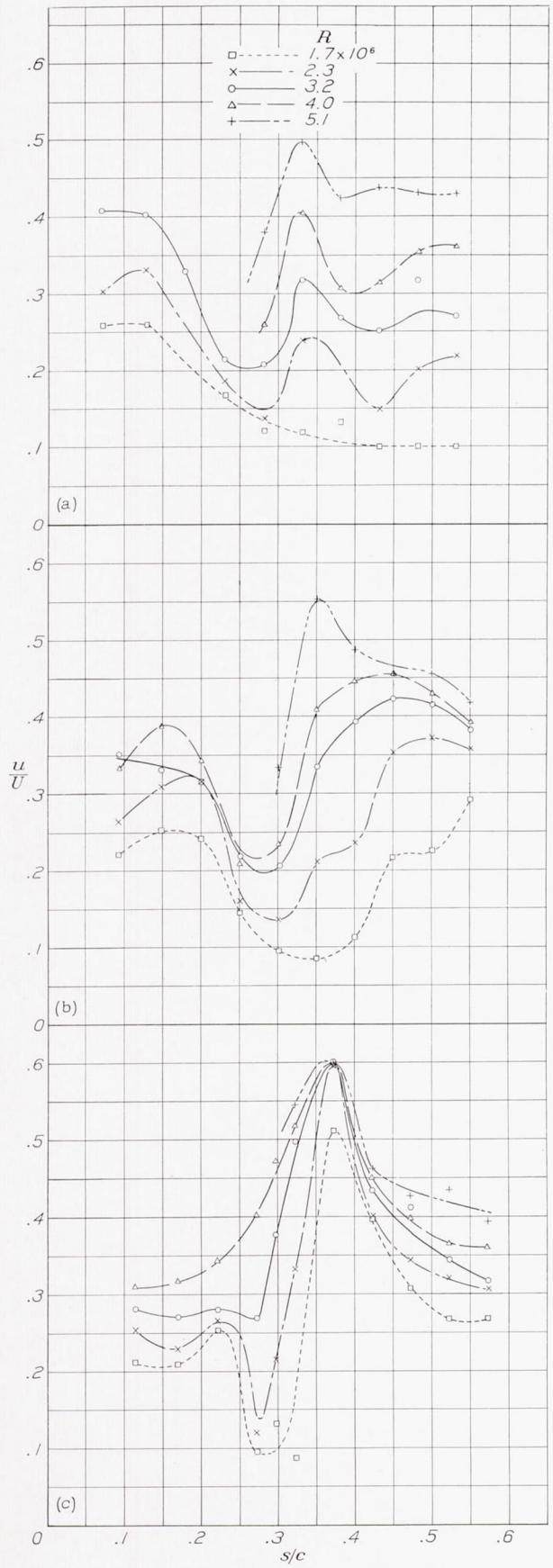

(a) $c_l=-0.47$. (b) $c_l=0$. (c) $c_l=0.49$.

FIGURE 24.—Boundary-layer velocities 0.008 inch above the upper surface of the NACA 0025 airfoil.

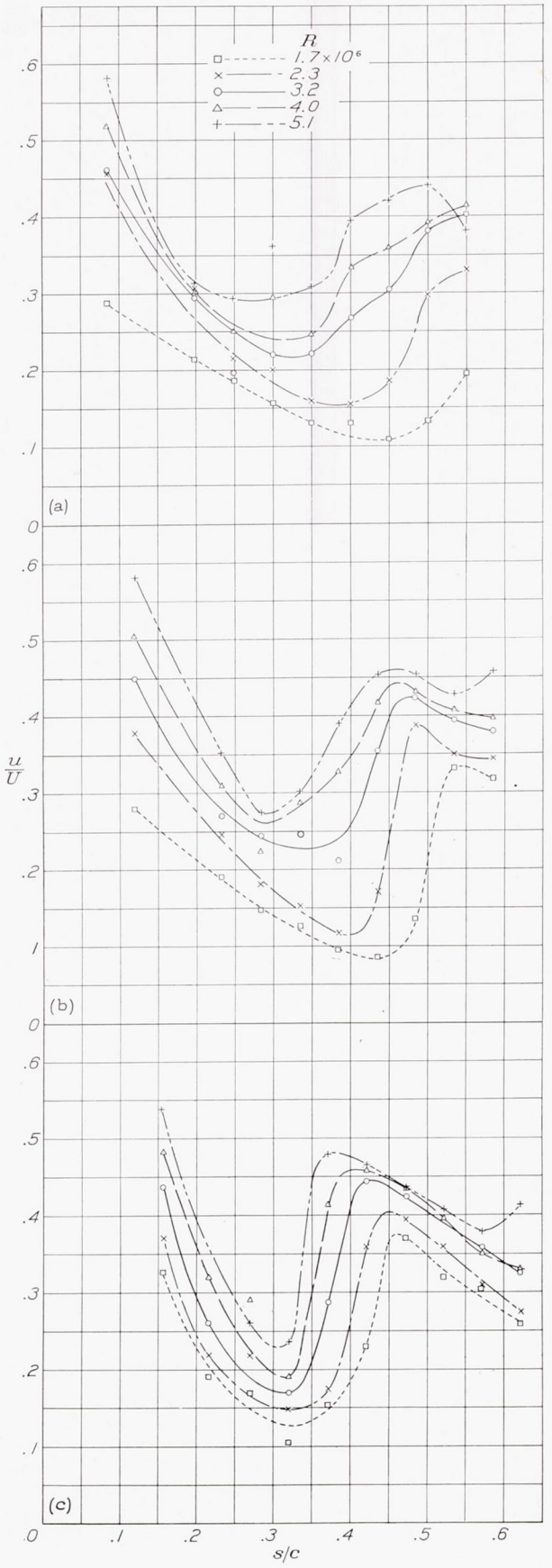

(a) $c_l=-0.33$. (b) $c_l=0$. (c) $c_l=0.35$.

FIGURE 25.—Boundary-layer velocities 0.008 inch above the upper surface of the NACA 0035 airfoil.

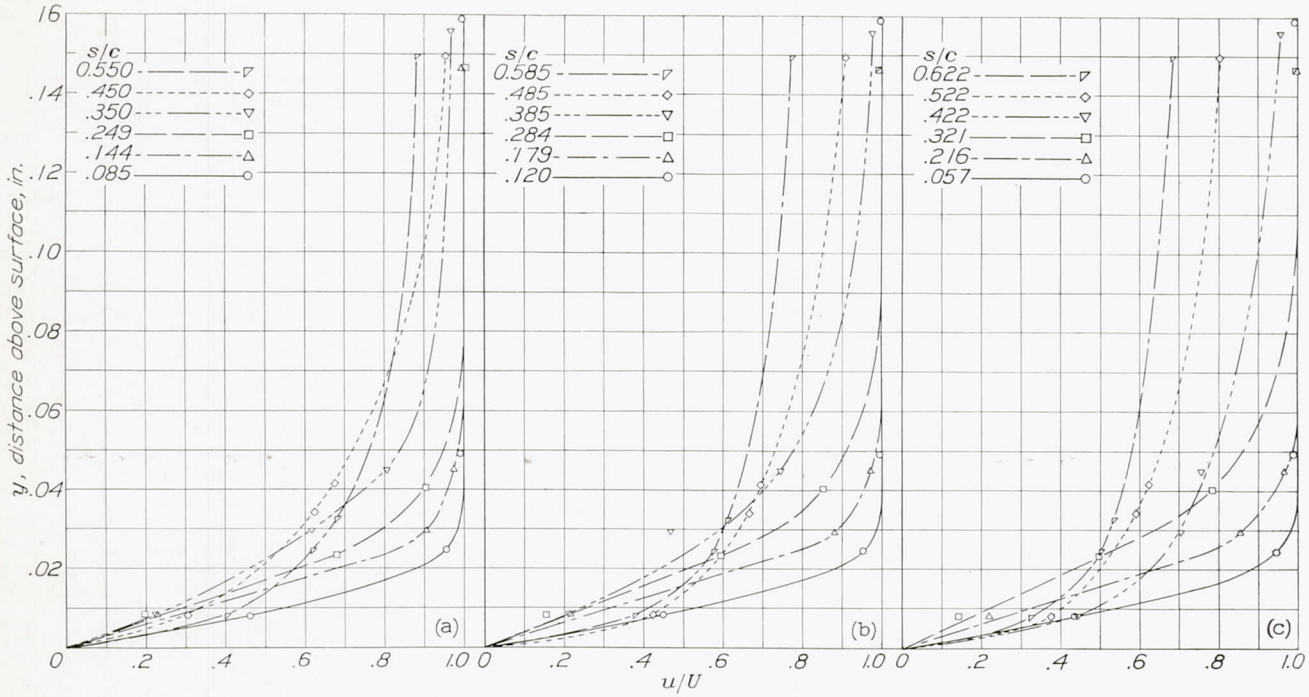

(a) $c_l = -0.47$. (b) $c_l = 0$. (c) $c_l = 0.49$.

FIGURE 26.—Boundary-layer velocity profiles at several chord positions on the NACA 0025 airfoil. Reynolds number, 3,200,000.

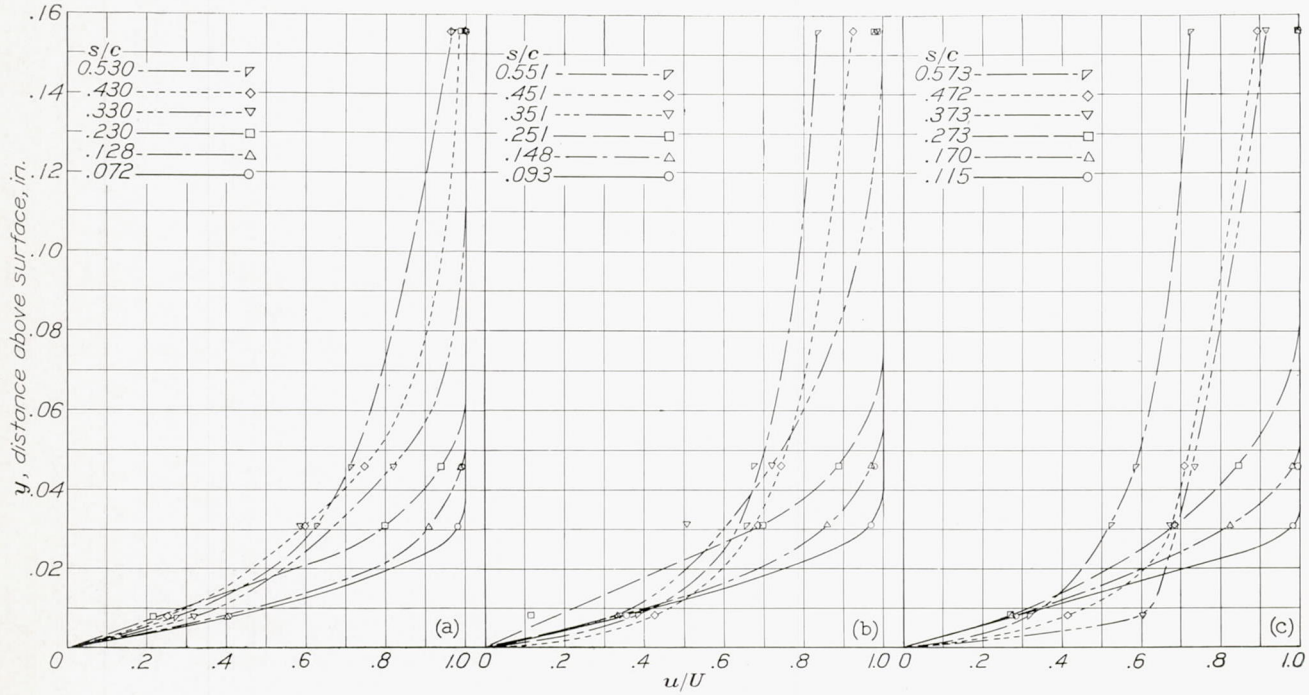

(a) $c_l = -0.33$. (b) $c_l = 0$. (c) $c_l = 0.35$.

FIGURE 27.—Boundary-layer velocity profiles at several chord positions on the NACA 0035 airfoil. Reynolds number, 3,200,000.

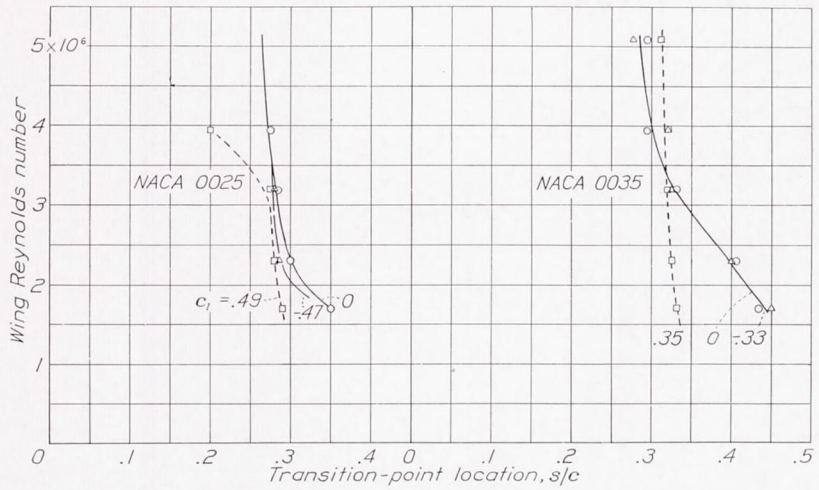

FIGURE 28.—Transition-point location on the upper surfaces of the NACA 0025 and 0035 airfoils as affected by lift coefficient and Reynolds number.

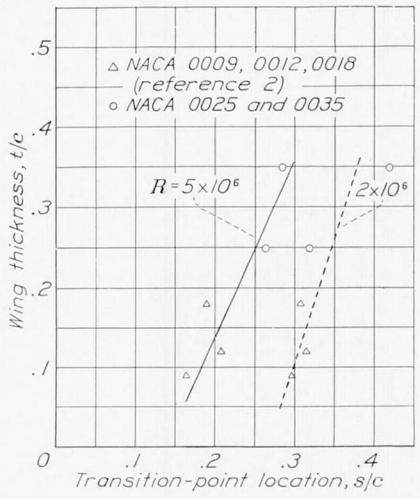

FIGURE 29.—Effect of airfoil thickness on the location of the transition point. c_l, 0.

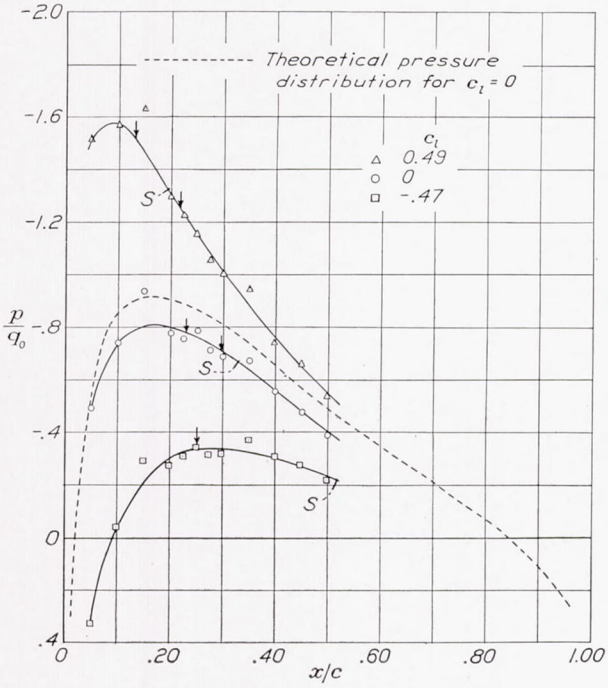

FIGURE 30.—Pressure distribution on the upper surface of the NACA 0025 airfoil for three section lift coefficients. Arrowhead ticks indicate the location of the transition points for Reynolds numbers of 1,700,000 and 4,000,000. The estimated laminar separation points are denoted by S.

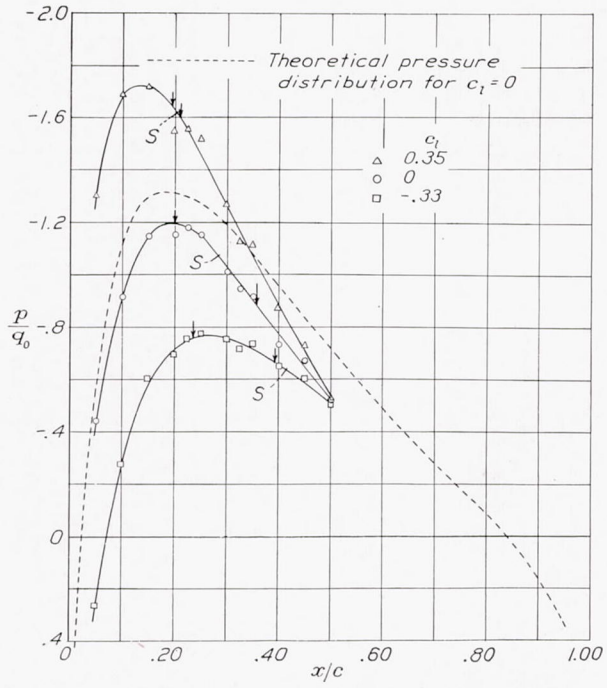

FIGURE 31.—Pressure distribution on the upper surface of the NACA 0035 airfoil for three section lift coefficients. Arrowhead ticks indicate the locations of the transition points for Reynolds numbers of 1,700,000 and 5,100,000. The estimated laminar separation points are denoted by S.

The variation of the transition-point location with Reynolds number for the two airfoils is given in figure 28. At low speeds, the forward movement of the transition points with increasing Reynolds numbers is quite rapid for the negative-lift and the zero-lift conditions. The position of the transition point for the NACA 0035 airfoil at the positive lift remains practically constant throughout the Reynolds number range investigated. There is also a slight movement for the NACA 0025 airfoil at a c_l of 0.49 up to a Reynolds number of 3,200,000, but from this point an increase in Reynolds number of 800,000 causes the transition point to move forward a distance equal to 7.5 percent of the chord.

The effect of airfoil thickness on the location of the transition point is presented in figure 29. Data from tests of the NACA 0009, 0012, and 0018 airfoils in the full-scale tunnel (reference 2) have been included in this figure. The curves indicate that transition takes place farther from the stagnation point as the airfoil thickness is increased.

The pressure-distribution determinations, which were obtained with the static tubes included in the banks of tubes for the boundary-layer surveys, are shown in

figures 30 and 31 for each of the test lift coefficients. The static-pressure-distribution curves for the NACA 0025 and 0035 airfoils at zero lift are parallel to but considerably lower than the theoretical curves. The discrepancy may be due to failure of conventional airfoil theory when applied to airfoils of these extreme thicknesses.

The transition-point location obtained at the highest and lowest the Reynolds numbers of the test is indicated on each of the pressure-distribution curves in figures 30 and 31. The laminar separation points, which are also indicated on the curves, were estimated by the method of reference 8. It will be noted that the separation points in most cases are not far distant from the points of transition.

CONCLUSIONS

Within the range covered, the section profile-drag coefficients of the NACA 0025 and 0035 airfoils were practically independent of Reynolds number, the values of these coefficients for the two airfoils being 0.0082 and 0.0112, respectively. With the airfoils equipped with 0.20c full-span split flaps and at a Reynolds number of 3,000,000, the maximum lift coefficient of the NACA 0025 airfoil was 2.57 and that of the NACA 0035 airfoil was 2.54. Tuft and momentum surveys indicated poor flow beginning at a low lift coefficient near the trailing edges of the NACA 0025 and 0035 airfoils. When based on the projected frontal area, the section with the lowest profile-drag coefficient was found to have a thickness approximately 30 percent of the chord.

LANGLEY MEMORIAL AERONAUTICAL LABORATORY,
NATIONAL ADVISORY COMMITTEE FOR AERONAUTICS,
LANGLEY FIELD, VA., *September 25, 1940.*

REFERENCES

1. Goett, Harry J., and Bullivant, W. Kenneth: Tests of N.A.C.A. 0009, 0012, and 0018Airfoils in the Full-Scale Tunnel. Rep. No. 647, NACA, 1938.
2. Silverstein, Abe, and Becker, John V.: Determination of Boundary-Layer Transition on Three Symmetrical Airfoils in the N.A.C.A. Full-Scale Wind Tunnel. Rep. No. 637, NACA, 1939.
3. Goett, Harry J.: Experimental Investigation of the Momentum Method for Determining Profile Drag. Rep. No. 660, NACA, 1939.
4. DeFrance, Smith J.: The N.A.C.A. Full-Scale Wind Tunnel. Rep. No. 459, NACA, 1933.
5. Platt, Robert C.: Turbulence Factors of N.A.C.A. Wind Tunnels as Determined by Sphere Tests. Rep. No. 558, NACA, 1936.
6. Silverstein, Abe, and Katzoff, S.: A Simplified Method for Determining Wing Profile Drag in Flight. Jour. Aero. Sci., vol. 7, no. 7, May 1940, pp. 295–301.
7. Stack, John, Lindsey, W. F., and Littell, Robert E.: The Compressibility Burble and the Effect of Compressibility on Pressures and Forces Acting on an Airfoil. Rep. No. 646, NACA, 1938.
8. von Doenhoff, Albert E.: A Method of Rapidly Estimating the Position of the Laminar Separation Point. T. N. No. 671, NACA, 1938.

TABLE I

IMPORTANT CHARACTERISTICS OF THE NACA 0009, 0012, 0018, 0025, AND 0035 AIRFOILS FROM FULL SCALE TUNNEL TESTS

[Data for the NACA 0009, 0012, and 0018 airfoils are from reference 3].

NACA airfoil	Reynolds number (millions)	Airfoil characteristics, aspect ratio 6						Section characteristics	
		$C_{L_{max}}$	α at $C_{L_{max}}$ (deg)	$\frac{dC_L}{d\alpha}$ (per deg)	$C_{D_{min}}$	$\left(\frac{L}{D}\right)_{max}$	$\Delta C_{L\,max}$ at δ_{flap} (1)	c_{d_0} at $c_l=0$	a_0 (per deg)
0009; rounded tips	2	1.09	16.4	0.070				0.0064	
	3	1.18	17.2	.070	0.0062	24.9	0.74	.0062	0.094
	4	1.23	17.6	.070	.0061			.0060	
	5	1.25	18.0	.070	.0060			.0059	
	6			.070	.0059			.0058	
	7			.070	.0057			.0057	
0012; rounded tips	2	1.21	17.9	.069				.0067	
	3	1.30	19.1	.069	.0067	24.7	.90	.0065	.094
	4	1.36	19.5	.069	.0066			.0064	
	5			.069	.0065			.0063	
	6			.069	.0064			.0063	
	7			.069	.0063			.0062	
0018; rounded tips	2	1.14	18.2	.068				.0080	
	3	1.23	18.8	.068	.0079	21.0	1.22	.0077	.094
	4	1.29	19.3	.068	.0077			.0075	
	5			.068	.0076			.0074	
	6			.068	.0074			.0072	
	7			.068	.0073			.0071	
0025; rounded tips	2	1.02	22.3	.062	.0088			.0085	
	3	1.03	21.2	.062	.0085	20.4	1.54	.0082	.082
	4	1.04	20.5	.062	.0085			.0082	
	5			.062	.0085			.0082	
	6			.062	.0085			.0082	
0035; rounded tips	2	.90	29.3	.044	.0118			.0115	
	3	.86	29.9	.044	.0115	16.4	1.69	.0112	.051
	4	.86	29.6	.044	.0115			.0112	
	5			.044	.0115			.0012	
	6			.044	.0115			.0012	
0012; square tips; 0.20c full-span split flap deflected 60°.	2	2.12	18.0	.066		5.2			
	3	2.21	19.4	.066					.096
	4	2.28	20.6	.066					
0025; rounded tips; 0.20c full-span split flap deflected 60°.	2	2.47	19.4	.075					
	3	2.52	20.2	.075		5.6			.11
	4	2.55	21.0	.075					
0035; rounded tips, 0.20c full-span split flap deflected 60°.	2	2.37	15.0	.082					
	3	2.44	16.0	.082		5.8			.11
	4	2.44	15.8	.082					

[1] Increment of lift due to 0.20c full-span split flap with flap set at angle giving greatest maximum lift. Values taken from faired curve (fig. 20).

TABLE II

DISTANCES ALONG THE UPPER SURFACE (s/c) FROM THE THEORETICAL STAGNATION POINT CORRESPONDING TO DISTANCES ALONG THE CHORD LINE (x/c) FROM THE LEADING EDGE OF THE TWO NACA AIRFOILS TESTED

x/c	NACA 0025 airfoil			NACA 0035 airfoil		
	s/c			s/c		
	$c_l=-0.47$	0	0.49	$c_l=-0.33$	0	0.35
0.00	−0.021	0	0.022	−0.035	0	0.037
.05	.072	.093	.115	.085	.120	.157
.10	.128	.149	.170	.144	.179	.216
.15	.179	.200	.222	.198	.233	.270
.20	.230	.251	.273	.249	.284	.321
.25	.281	.302	.323	.300	.335	.372
.30	.330	.351	.373	.350	.385	.422
.35	.380	.401	.423	.401	.436	.473
.40	.430	.451	.472	.450	.485	.522
.45	.480	.501	.523	.500	.535	.572
.50	.530	.551	.573	.550	.585	.622

U. S. GOVERNMENT PRINTING OFFICE: 1941

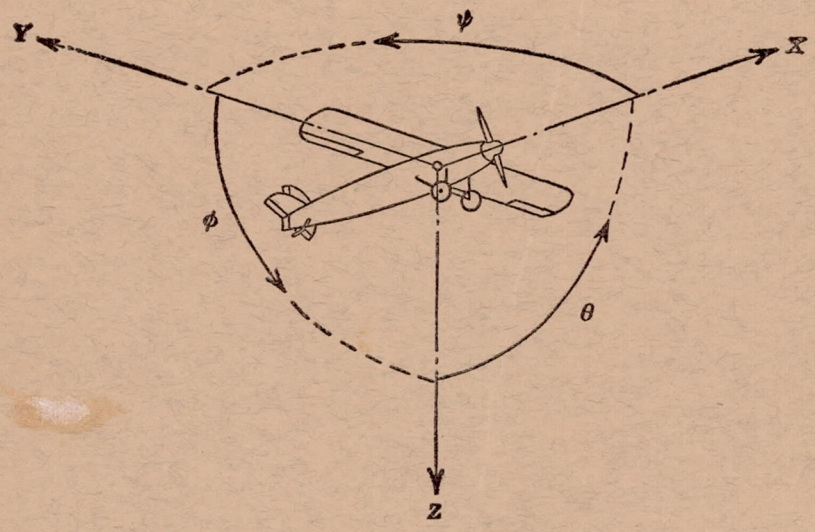

Positive directions of axes and angles (forces and moments) are shown by arrows

Axis		Force (parallel to axis) symbol	Moment about axis			Angle		Velocities	
Designation	Symbol		Designation	Symbol	Positive direction	Designation	Symbol	Linear (component along axis)	Angular
Longitudinal	X	X	Rolling	L	$Y \longrightarrow Z$	Roll	φ	u	p
Lateral	Y	Y	Pitching	M	$Z \longrightarrow X$	Pitch	θ	v	q
Normal	Z	Z	Yawing	N	$X \longrightarrow Y$	Yaw	ψ	w	r

Absolute coefficients of moment

$C_l = \frac{L}{qbS}$ (rolling) $\quad C_m = \frac{M}{qcS}$ (pitching) $\quad C_n = \frac{N}{qbS}$ (yawing)

Angle of set of control surface (relative to neutral position), δ. (Indicate surface by proper subscript.)

4. PROPELLER SYMBOLS

D Diameter

p Geometric pitch

p/D Pitch ratio

V' Inflow velocity

V_s Slipstream velocity

T Thrust, absolute coefficient $C_T = \frac{T}{\rho n^2 D^4}$

Q Torque, absolute coefficient $C_Q = \frac{Q}{\rho n^2 D^5}$

P Power, absolute coefficient $C_P = \frac{P}{\rho n^3 D^5}$

C_s Speed-power coefficient $= \sqrt[5]{\frac{\rho V^5}{P n^2}}$

η Efficiency

n Revolutions per second, rps

Φ Effective helix angle $= \tan^{-1}\left(\frac{V}{2\pi r n}\right)$

5. NUMERICAL RELATIONS

1 hp = 76.04 kg-m/s = 550 ft-lb/sec

1 metric horsepower = 0.9863 hp

1 mph = 0.4470 mps

1 mps = 2.2369 mph

1 lb = 0.4536 kg

1 kg = 2.2046 lb

1 mi = 1,609.35 m = 5,280 ft

1 m = 3.2808 ft